Saimaa University of Applied Sciences
Faculty of Technology, Lappeenranta
Degree Programme in Mechanical Engineering and Production Technology

Georgii Sokolov

Analysis of electrodynamic brake for utilization in systems with rotating shafts

Thesis 2016

Abstract

Georgii Sokolov
Analysis of electrodynamic brake for utilization in systems with rotating shafts, 52 pages
Saimaa University of Applied Sciences
Faculty of Technology Lappeenranta
Degree Programme in Mechanical Engineering and Production Technology
Thesis 2016
Instructor: Senior Lecturer Simo Sinkko, Saimaa University of Applied Sciences

The goal of this study was to conduct an analysis of an opportunity to apply eddy current brakes in dynamical systems containing rotating shafts. While conducting the research the general principles of deceleration, eddy currents' origin, basics of magnetism and currently existing types of brakes were clarified and gathered briefly, but informatively.

The theory which is explained in this thesis was taken from reliable secondary sources. The concepts of physics were investigated from several student books, however, a particular field of eddy current brake application was studied in terms of academic articles ranging from the 1940s up to the present.

Additional empirical data needed to complete estimations of designed system was combined following the specification sheets of various industrial companies.

The output of the research can be described as a dynamically estimated model the characteristics of which are based on real prototype and adjusted to act effectively within prototype's environment. Based on system's preliminary sketch, a general understanding of braking disk mounting and electromagnets internal organization can be studied and developed further. The numerical investigations gave a short presentation of physical and dynamical effects caused by eddy current brake operation.

Keywords: Eddy-current brake, ECB, electrodynamic brake, rotating shafts, brakes, sustainable solutions development, application of eddy-current brake, wind turbine brake development.

Table of Contents

List of abbreviations and symbols

EMF	electromotive force
AC	alternating current
DC	direct current
ECB	eddy current brake
v	speed [m/s]
$\mathcal{E}$	EMF [Volts (*V)*]
R	material's internal resistance [Ohm]
Φ	magnetic flux [Wb/m^3]
t	time [second]
$d\Phi$	variation of magnetic flux
dt	variation of time
$\underset{B}{\rightarrow}$	induction [Wb]
I_{ed}	eddy current [A]
F_m	magnetic force = F_A [N]
l	invariable geometrical parameter of a moving conductive body [m]
A	area [m^2]
N	number of turns in a coil
I	electric current of circuit [A]
μ_0	permeability of free air (4π * 10^{-7} Hm^{-1})
l_g	mean length of flux path [m]
D	diameter of a magnet core [m]
d	thickness of rotating disk [m]
R	effective radius of the disk [m]; reluctance [At/Wb] (Equation 7.5)
$\dot{\Theta}$	angular velocity of the disk [rad/s]
σ	specific conductivity of the material [1/Ohm*m]
γ	electric conductivity [S/m]
ω	angular velocity [rad/s]
h	height [m]
S	reluctance [At/Wb]
L	inductance of a coil [H]
W	energy of a coil [J]
i	excitation current of a coil [A]
T	torque [N*m]
E	electric field intensity [N/C]
ρ	resistivity of the material [Ohm *m]; (equation 8.3) density [kg/m^3]
δ	sheet thickness [m]
τ	braking torque [N*m]
m	mass [kg]

1 Introduction

1.1 Goal of the project

The aim of the thesis includes theoretical research concerning the mechanical effect caused by eddy currents in the rotating conductive disk and a study regarding the effectiveness to use eddy current disk brakes in wind power turbines for purposes of rotational speed control. The experimental data is requested from LUT energy department, which owns wholly operated 26 kW power and 36 meters in height wind turbine for educational and research purposes shown in Figure 1.1 (LUT Wind Power).

Figure 1.1. Wind Turbine (LUT).

1.2 General principles of deceleration

A great number of technical literature is devoted to the braking of machines and devices. Despite the complicity of the research, braking devices can be divided into two groups following the principle of braking force origin.

In the first group or the group of friction brakes, an effect appears as a result of a physical contact between moving and stationary parts. Due to the physical touch, kinetic energy transforms into thermal energy and dissipates as heat.

The group of friction brakes can be classified as it is illustrated in Table 1.1:

Classification	Sub-group
Braking element principle	a. Plate b. Band c. Disk d. Conical e. Railway (Linear)
Structure arrangement	a. Closed b. Open c. Combined
Actuation Principle	a. Automatic b. Controlled
Drive type	a. Electromagnetic b. Electrohydraulic c. Electromechanical d. Pneumatic e. Mechanical

Table 1.1. Generalized classification of friction brakes (Ozolin 2009)

In the second group, braking effort is produced without the mechanical contact but by the interaction of electric and magnetic fields. Such kind of braking is called electrodynamic or eddy current braking. The types of electrodynamic braking devices are divided regarding a source of magnetic field. The source of the magnetic field can be chosen as either a permanent magnet or an electromagnet.

Permanent magnets were applied in technical application since 1831 when Faraday discovered appearance of electromagnetic induction: he noticed that current appears in a conductive circuit when the circuit relocates about a magnet or in relation to another current conducting circuit. From 1832 permanent magnets were utilized in a vast number of applications but, eventually, they were substituted with electromagnets according to their better energy and mass characteristics.

Besides that, development of permanent magnets continues as they became popular in applications where an independence from a power source is important. Permanent magnets are used in linear electrodynamic brakes, which are

frequently utilized in a high-speed application such as trains and even a roller coaster. Linear electrodynamic brake is usually attached either to the surrounding objects or to the moving body. In its stationary application, that kind of brakes are set on underlying railway tracks to supply the train with efficient and dynamic braking in front of the station or along the emergency side tracks to dissipate most of the rail transport's kinetic energy. Quite frequently linear brakes are also met in the condition when they are attached to a moving body. In both cases, the combination with electromagnets is also presented.

Electromagnets compared to the permanent magnets have a feature that their magnetic field can be supplied and controlled by an electric current despite the magnetic characteristic of a core material. Electrically controlled magnets are usually associated with the limited space applications where it is inconvenient to design systems with approaching and leaving magnets.

Nowadays, different approaches are used to estimate a behavior of a conductive body under an impact of the magnetic field. For example, Guru and Hiziroglu (1998) highlight Maxwell's second equation to specify an electric field intensity at a fixed point in space when a magnetic field is a function of time.

2 Eddy Currents

Eddy currents are the electric currents induced in the conductive body, which moves through a magnetic field and, therefore, undergoes a change of the flux over a limited period. A closed-loop circuit appears in the depth of the conductor. As it is published, electrical current is determined as a rate of charged particles through a considered cross-sectional area (Tipler, 1990). The statement carries out a fact that a particular force might cause a charged particle to flow and, by that, to form an electrical current. That particular effect is called electromotive force (EMF) and measured in volts as same as the unit of potential difference.

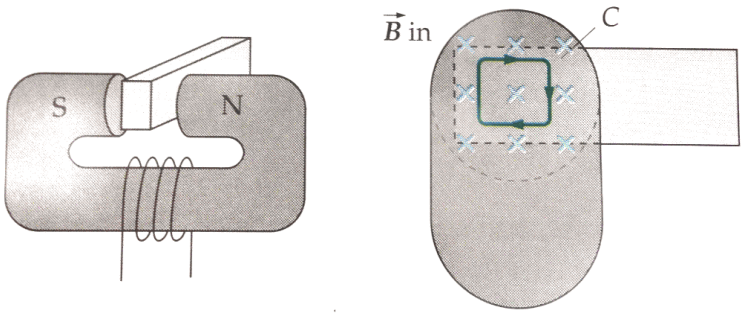

Figure 2.1. Conductive material is placed between two poles of an electromagnet (Tipler 1990).

The EMF of induction that initiates eddy currents arises following both Faraday's law of induction and Lenz's law. In a brief explanation, experiments held by Faraday showed that any change of a magnetic flux within an area surrounded by a conductive circuit will initiate an EMF similar in magnitude to the rate of magnetic flux change. Additionally, Lenz's law states that a polarity of the induced EMF is such that it initiates a current whose magnetic field resists the change that produced them. (Tipler 1990. p. 929, 933.)

On the left, Figure 2.1 gives a simple example of how eddy currents occur in a stationary conductive slab. From the picture above, it is seen that a piece of a metal is placed between the poles of an electromagnet, which is connected to an electric circuit supplied with AC.

As it is stated that the system's power source is an AC source, an amount of induction *B* extracted into the gap between the poles continuously varies according to variable current flow. The amount of induction directly affects the magnitude of magnetic flux due to its dependency (Tipler, 1990. p.928). If the magnetic flux is subjected to a change over the time, EMF is induced in a conductive body following Faraday's law of induction and Lenz's law determines the direction of the induced EMF.

On the right of Figure 2.1, a detailed scheme of the induced eddy currents and penetrating induction is captured. An indicated loop *C* is only one of many possible loops that occur in the conductor. Due to the Lenz's law, the direction of the current in loop *C* must be so that it induces its own magnetic field to resist the change in the primary magnetic field B_{in} of the electromagnet. At the moment captured in Figure 2.1, the vector of induction is forwarded into the paper, but the

intensity of the flow is decreasing. Applying the right-hand rule explained in Figure 2.2, it is determined that induction created by the circular loop rebels against the change trying to add some intensity in the direction of B_{in}.

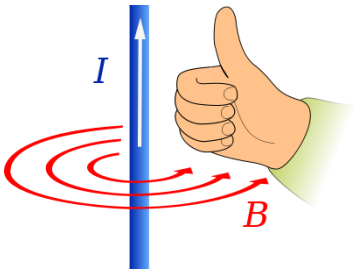

Figure 2.2. Right-hand rule application (Wikipedia 2016).

On the other hand, as the power source has AC characteristics, after one fourth of the period the loop C will change its direction and become counterclockwise.

That is the basics of eddy currents origin as they appear in stationary objects under a stream of the magnetic field.

The magnitude of eddy current following Ohm's law is equal to the dependency of induced EMF to resistance of material (Formula 2.1)

$$I_{ed} = \frac{\mathcal{E}}{R} = -\frac{1}{R}\frac{d\Phi}{dt} \quad (2.1)$$

Therefore, it is claimed that the less electrical resistance material has, the more magnitude of the current is. Minus sign means that the current always goes so as to create induction with opposite direction with respect to magnetic flux change (Tipler 1990).

3 Consequences of Eddy Currents

Eddy currents are frequently unwanted due to the loss of energy they cause. In such systems as described in table 1.1, an electrical power tends to disappear in a form of dissipated heat that is produced by the circular currents. It was firstly noticed by a French physicist Leon Foucault, so eddy currents are usually named after him as Foucault currents.

Power loss caused by the currents can be reduced by the increase in resistance of the system's material or structure to form the paths for circulating currents. Two methods can be applied to eliminate high magnitudes of eddy currents as pictured in the following Figure 3.1. (Tipler, 1990. p.939).

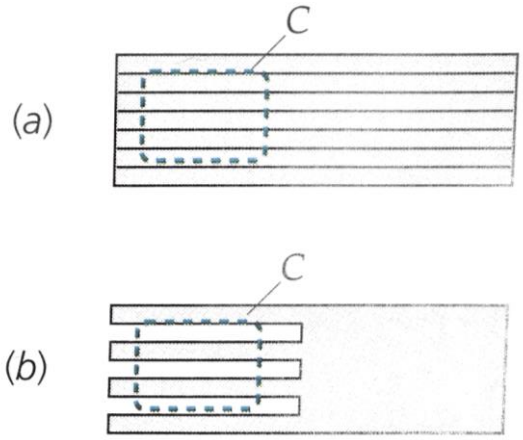

Figure 3.1.Reduced eddy currents in a metal slab. (Tipler 1990, p.939)

Figure 3.1 (a) shows that a workpiece can be laminated, consisting of thin strips stuck together. In case (a) eddy currents are limited by the glue which is non-conducting, thus, a power consumed by EMF is much less compared to a solid state situation. On Figure 3.1 (b) more eradicative method is illustrated: surface area, which is subjected to the changing magnetic flux, is performed in a shape of a comb to have air as an isolating layer. These methods are implemented to reduce heating and a drag of a magnetic force which will be described later in the following chapter. (Tipler, 1990. p.939)

Circular currents also convert energy when it is functionally required and, therefore, they might be objectionable. Eddy currents are used in machinery as well as in daily life. For example, induction stoves use the principle of induction to make food cooked transmitting electrical energy into a thermal one, at the same time keeping the stove burners cool, thus, it is safe for children and pets to be around.

However, eddy currents allow converting the energy into heat not only from electrical but also from mechanical energy. As an instance to that, the use of eddy currents in elevator's industry is underlined preventing fatal accidents when hawsers are torn. With a help of electromagnetic induction, the elevator is decelerated gradually before touching the ground.

A process of electrical energy conversation into heat was briefly described in the chapter above. The next paragraphs will be dedicated to giving an overview of how the mechanical energy can be transmitted into heat with its further elimination.

3.1 Electrodynamic deceleration

A physical existence of eddy currents can be seen in the explanation of Figure 3.2. The initial information of the system differs with the previous example from Figure 1.1 by the condition that electrical circuit is a circuit of a direct current (DC) and, therefore, induction B_{in} is same over time.

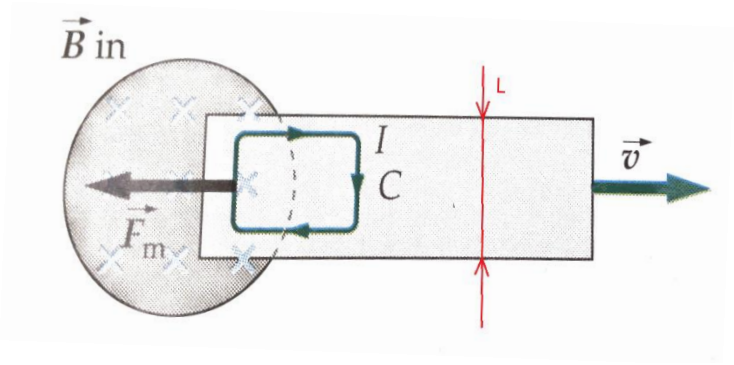

Figure 3.2. Physical demonstration of eddy currents (Tipler, 1990. p.939).

Despite the fact that magnitude of induction is constant, a change in magnetic flux happens because an object moves through a magnetic field with a speed *V* as shown. In Figure 3.2 generated EMF is proportional to the magnetic flux change, like Faraday's law states, but at the same time can be described via other parameters: *V* – speed, *B* – induction and *l* – the height of an area in which *B* penetrates. (Tipler, 1990. p.936).

$$\mathcal{E} = \frac{d\Phi}{dt} = (v \times B)\, l \qquad (3.1)$$

Lenz's law forecasts the direction of motional EMF so as eddy current caused by the motional EMF is opposing the change in magnetic flux that creates it. In Figure 3.2 magnetic flux tends to decrease as an area *A,* through which induction *B* penetrates, is decreasing (Formula 3.2).

$$\Phi = B * A \qquad (3.2)$$

As magnetic flux decreases, a magnetic field created by eddy current tries to resist changes and has a direction in the paper, similar to the magnetic field of a magnet. Thus, following the rule in Figure 2.2, clockwise direction of eddy currents is determined.

As a conductor with the circulating current is moved within the magnetic field as illustrated in Figure 3.2, Fishbane, Gasioriwicz & Thornton (1996) claim that magnetic force or Ampere's force always acts on the current induced in a conductor so that it inhibits any motion that produced it. (Fishbane, P. M., 1996. p. 847)

A magnetic force applied to a current carrying conductor situated in a magnetic field called Ampere's force, and its direction is estimated with a left-hand rule as described in Figure 3.3.

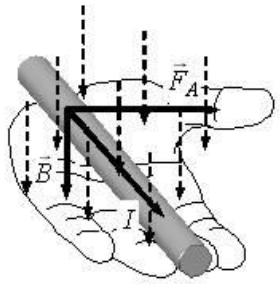

Figure 3.3. Left-hand rule (PhysBook 2011).

From Figure 3.2 it is seen that a force F_m (magnetic force) or F_A (Ampere's force) acting on a current which is placed under the steam of induction B is determined by the left-hand rule and forwarded to the right.

The kinetic energy of a conductor is dissipated as heat produced by eddy currents. Thus, conversation from kinetic energy to its thermal state happens.

3.2 Drag force factors

The section explains what the characteristics are that might affect an impact applied to a conductive body moving in a magnetic field. Among them are:

Speed

An object's velocity through a magnetic field directly affects the magnetic force exerted on it. Figure 3.2. The dependency from speed is correct for the forces on induced eddy currents due to motional EMF because their origin is also proportional to the speed as described by Formula 2.

Material

A force might be carried to an extreme by taking a body's material with as little resistance as possible to get the highest magnitudes of eddy currents. Formula 1 illustrates a dependency between an induced current and material's resistance in which the currents are induced.

Direction

As it can be observed from Formula 2, one of the essential conditions for a counterforce to occur is that the vector of *V* and vector induction *B* are not parallel to each other. Taking that statement into account it is supposed that the maximum braking force can be achieved by setting the vectors in perpendicular directions.

4 Types of brakes

In nowadays-technical applications, two main types of eddy current brakes are utilized. Those are the linear type and disk type of brakes. They both share the same principle when a decelerating conductor is moved through a magnetic field, but still there are some features, which differ them.

Figure 4.1. A series of magnets mounted along the railway track (Coastersandmore 2010)

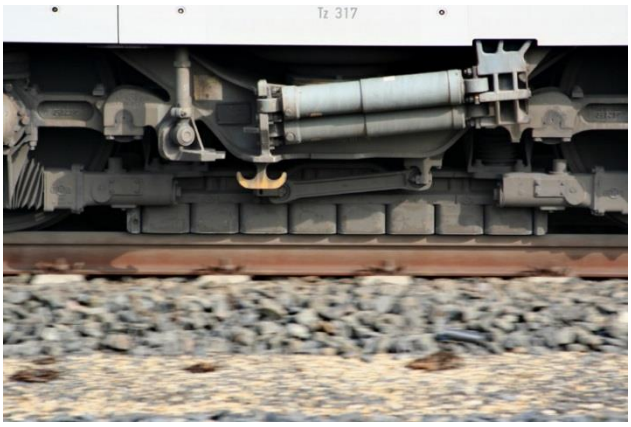

Figure 4.2. Linear brake attached to a moving object. (Wikipedia 2016)

Linear eddy current brakes usually consist of permanent magnets to be independent of a source of power, but as it was written in the section about the deceleration of machines, electromagnets are also used but preferably in mounted-on-object condition.

As Figure 4.1 illustrates, the magnets are mounted on the railway track covering a certain area, Figure 4.2 gives a brief overview of how eddy current linear brakes look when they are attached to a train.

4.1 Eddy current disk brakes and its features

Electrodynamic disk brakes are similarly utilized in the high-speed railway industry. For example, a Japanese high-speed manufacturer has actively adapted an effect of electrodynamics to slow down 700 series Shinkansen train. The disk typically consisting of non-ferromagnetic material is situated between the poles of an electromagnet which is controlled from the control cabin. Braking effort is varied by a magnitude of the electric current which supplies magnets, variations in the braking effort is an advantage considering the sphere of application. Nevertheless, the material of the disk is situated under the magnetic field much more frequently compared to the linear brake. That is a consequence of areas difference. Due to the small surface area of the circular disk, eddy current disk brakes are heated much harder than its linear analog.

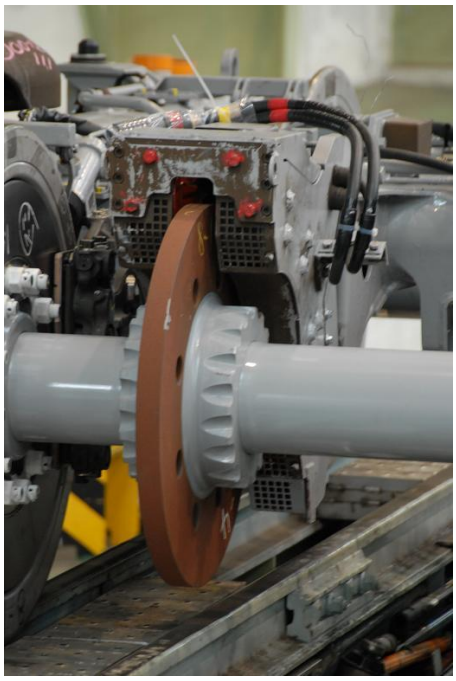

Figure 4.3. High-speed train disk brake (Wikipedia, 2016).

Among the specific features of eddy current disk brakes can be recalled:

- Temperature rise
- Dynamic deceleration. Braking torque is proportional to a change in magnetic flux over time, thus, depending on speed
- Inoperability when the derivation of flux by time is zero, therefore, speed is zero.

5 Magnetism

5.1 Magnetic fields

Description of the magnetic field shall be started with an explanation of a permanent magnet. The permanent magnet is a piece of ferromagnetic material, such as iron or nickel, which tends to attract other pieces of these materials.

The permanent magnet is shown in Figure 6.1. Originally, it has south and north poles and circulating lines of magnetic field between them following the direction from N to S. (Bird 2014)

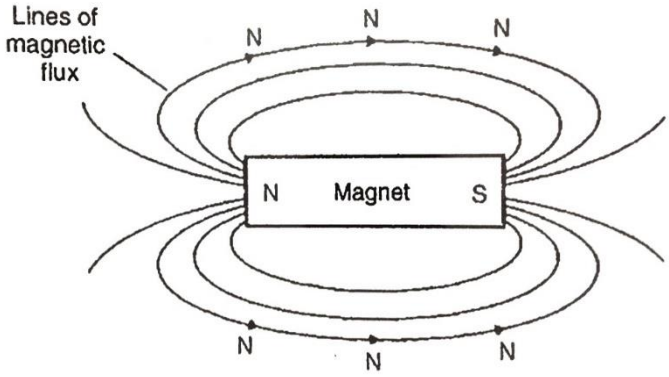

Figure 5.1. A sketch of magnetic field around a permanent magnet (Bird 2014).

Magnetic field around a permanent magnet is determined by several characteristics:

1. *Magnetic flux (Φ)* – the amount of force lines produced by a source. Measured in Weber [*Wb*].
2. *Magnetic flux density (B)* – the amount of flux passing through a fixed area. It relates to magnetic flux with the following Formula 5.1. Measured in Tesla [*T*]

$$B = \frac{\Phi}{A} \quad (5.1)$$

3. *Magnetomotive force (MMF) (F_m)* – the cause of the existence of magnetic flux in a circuit. Measured in Amperes and calculated with Formula 5.2.

$$F_m = NI \ (5.2)$$

4. *Magnetic field strength (H)*

$$H = \frac{NI}{l} \ (5.3)$$

(Bird 2014)

Therefore, the general relationship between *mmf* and magnetic field strength is:

$$mmf = NI = Hl \ (5.4)$$

The following concepts are considered, taking into account characteristics of materials:

1. Permeability (μ) – measure of how the material supports the formation of the magnetic field within itself (Wikipedia 2016). Measured in Henries per meter [H/m].

   The relationship between the strength of magnetic field and the magnetic flux density could be found using the constant of permeability (permeability of free space) μ_0.

   $$\frac{B}{H} = \mu_0 \quad (5.5)$$

   For other media, the relationship involves an additional variable μ_r

   $$\frac{B}{H} = \mu_0 \mu_r \quad (5.6)$$

   , where

   $$\mu_r = \frac{flux\ density\ in\ material}{Flix\ density\ in\ vacuum} \quad (5.7)$$

   Such tools as B-H curves are useful to see measured values graphically. The B-H curve also shows a gradual saturation of the material depending on its properties (Figure 5.2). Magnetic saturation of the material is the state of a material when an increase in the external magnetic field strength *H* cannot increase the magnetization of the material further, so magnetic flux density *B* is graphically straightening (Wikipedia 2016).

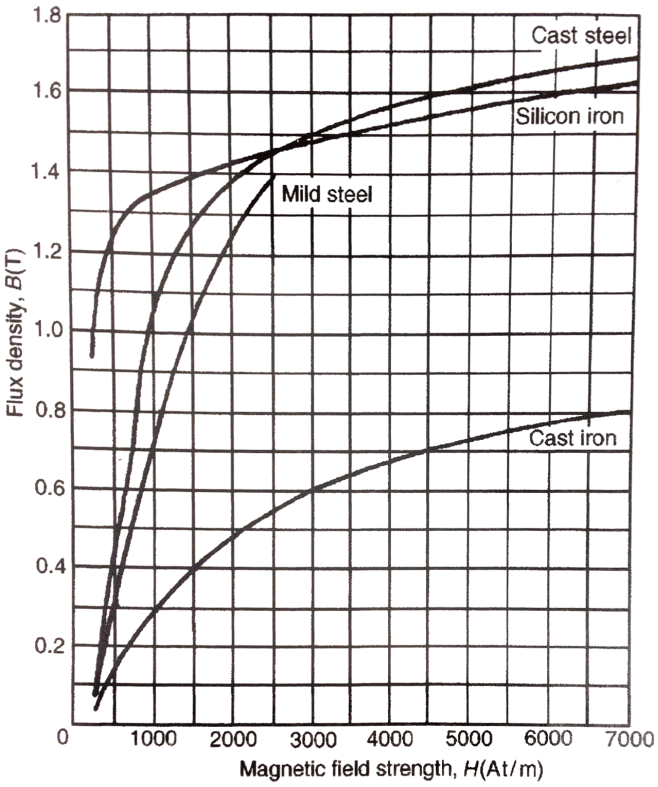

Figure 5.2. B-H curves for four materials (Bird 2014)

2. Reluctance S (R_M) – the magnetic resistance of a magnetic circuit to the presence of magnetic flux.

$$S = \frac{F_M}{\Phi} = \frac{l}{\mu_0 \mu_r A} \quad (5.8)$$

Electrical circuit		Magnetic circuit	
e.m.f. E	(V)	mmf F_m	(A)
current I	(A)	flux Φ	(Wb)
resistance R	(Ω)	reluctance S	(H^{-1})
$I = \frac{E}{R}$		$\Phi = \frac{\text{mmf}}{S}$	
$R = \frac{\rho l}{A}$		$S = \frac{l}{\mu_0 \mu_r A}$	

Figure 5.3. Comparison between electrical and magnetic quantities (Bird 2014).

(Bird 2014)

However, magnetic field also can be set up by electric currents. The lines of magnetic flux surround the conductor according to the screw rule as pictured in Figure 2.2. Furthermore, with a presence of electric current in a wire bent in a shape of a solenoid, a magnetic field similar to the one of a permanent magnet is born (Figure 5.4).

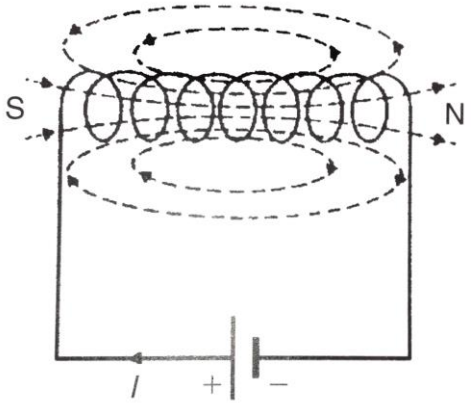

Figure 5.4. Magnetic field of a solenoid (Bird 2014).

The solenoid is vital in electromagnetism. Since the magnitude of the magnetic field depends on the current inside a solenoid, then the magnetic field can be adjusted by controlling the flow of current. An Electromagnet based on the solenoid has provided many applications in electrical equipment. (Bird 2014)

5.2 Electromagnetic induction

Electromagnetic induction is a phenomenon when an EMF, thus the current is induced in an electrically conductive body due to the relative movement of the body and magnetic field (Bird 2014).

The major laws of induction are described by Faraday and Lenz, which was already discussed earlier in this thesis. The magnitude of EMF induced due to the relative motion of a conductor in a magnetic field is described in Formula 5.9. (Bird 2014)

$$\varepsilon = Blv \quad (5.9)$$

5.3 Inductance

Inductance is the property of a circuit to produce EMF through a change of flux initiated by a change of electrical current. It is also measured in volts and determined by following formula 5.10:

$$E = -N\frac{d\Phi}{dt} = -L\frac{dI}{dt} \quad (5.10)$$

Inductance of a coil (*L*) in Henrys [H]

$$L = \frac{N\Phi}{I} = \frac{N^2}{S} \quad (5.11)$$

After the inductance of coil is known, the energy store in a coil is calculated with Formula 5.12 and measured in joules [J]:

$$W = \frac{1}{2}LI^2 \quad (5.12)$$

(Bird 2014)

6 Eddy current brakes ECB

A basic eddy current brake is described as a conductor that moves through a magnetic field (Gosline 2008). As it was explained earlier in this paper, moving conductor loses its kinetic energy which is transferred into dissipating Joule heating with a help of circularly flowing currents as a reason of induced Lorenz force.

Plenty of research has been done to analyze and design systems implementing the effect of eddy currents including haptic or damping applications. In general, it could be stated that eddy current brakes carry the tendency of an angular velocity depending on braking torque.

As it is assumed by Andrew Gosline (2008), the relationship between geometrical, magnetical and electrical parameters to determine braking torque is described by Formula 6.1:

$$\tau_{diss} = n\frac{\pi\sigma}{4}D^2 dB^2 R^2 \dot{\theta} \quad (6.1)$$

The equation correctly describes the behavior of the torque at low speeds and shows that the retarding torque varies linearly with an angular velocity (Gosline 2008).

However, further investigations show that generated flux by eddy currents acts against the flux of magnetic circuit. It means at the time the disk reaches certain rotational speed, the induction of magnetic circuit will be entirely canceled by the induced counter induction. The moment after which the braking torque stops increasing is determined by the critical speed of the disk, introducing such characteristic as critical torque. (Caldwell & Taylor 1998)

Equation 6.2 is applied to determine the critical speed.

$$V_c = \frac{2}{\sigma\mu_0 d} \quad (6.2)$$

From the graph presented in Figure 6.1, it is observed that the braking torque increases linearly with the speed, but as soon as the critical speed is reached, the retarding torque decreases. Caldwell and Taylor refer to Wouterse's study to explain Figure 6.1 and provide an explanation referring to an asymptotical behavior at the critical speed region claiming that counteracted magnetic flux and induced back EMF act on the braking torque negatively. (Caldwell & Taylor 1998)

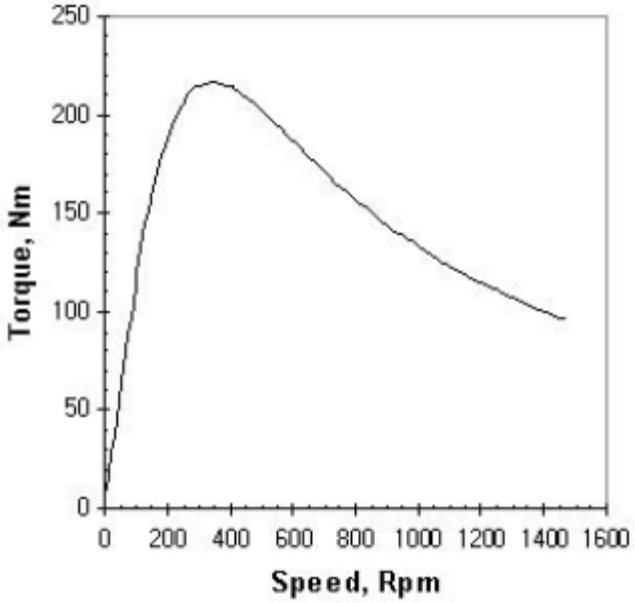

Figure 6.1. Mathcad model torque/speed curve, 10A coil current (Caldwell & Taylor 1998).

Theoretically, ECB can be expressed through the magnitude of current also. As it is described in Formula 6.3, the amount of Joule heating depends on a factor of electric conductivity and the magnitude of electric field. (Simeu & Georges 1995)

$$E = v \times B \quad (6.3)$$

According to Kapjin Lee & Kyihwan Park (1998), the magnitude of induction is described by a number of turns in a coil, applied current, a distance of air-gap and permeability of air (formula 6.4).

$$B = \frac{\mu_0 N i}{l_g} \quad (6.4)$$

Generally, the following assumptions are made as the literature review has been conducted:

- At low speed, the behavior of torque-angular velocity pair is linear due to the small magnitude of induction induced by eddy currents compared to the original.

- Critical speed region is a moment when a conductive element undergoes maximum magnitude of braking torque; the counter induction caused by eddy currents is not negligible anymore compared with B_0.
- In the region with speeds higher than a critical one, the mean of magnetic induction decreases further. As the Wouterse's experiments (1991) show, with further increase of angular speed to an infinite value, the original magnetic field will be completely canceled by the induction of induced currents.

(Wouterse 1991, p. 155)

6.1 Models

Among the majority of articles and presented physical approaches to estimate an effect which is caused by eddy currents in moving conductor, three essential mathematical models have been developed by Wouterse (1991), Smythe (1942) and Schieber (1974).

Initially, the problem of the eddy current brake was investigated by Rudenberg, who took a cylindrical machine as a starting point to design the brake that was assigned to be energized with DC. He supported the idea to place the poles of the magnets near each other, so the magnetic fields and current patterns are to be described with sinusoidal functions. (Wouterse 1991)

As all the power from rotational movement is dissipated into a thin (comparable to the structure) disk, the main problem of ECB is overheating of the braking disk. Therefore, a safe, reliable and sustainable system of cooling is required. (Wouterse 1991)

Smythe continued the work of Rudenberg by studying the eddy current distribution in a conductive rotating disk placed in magnetic field. Smythe's result is satisfactory at low-speed region but was inaccurate in the region of high speed. (Wouterse 1991)

Schieber has come up with the same dependencies and result as Smythe did, but extended the theory so as it additionally became valid for linearly moving strip. Schieber hasn't investigated the high sped region. (Wouterse 1991)

Taking the works of Smythe and Schieber into consideration, Wouterse tried to inquire into the high-speed regions as well as to prove the findings relating the low-speed region. Many of the people mentioned above have discovered similar phenomena that the behavior of torque in relation to speed was asymptotical closer to the high-speed region. (Wouterse 1991)

Smythe's analysis gives an exact explanation of conductive disk behavior at low-speed region utilizing the brake with permanents magnets. Smythe claims that usage of electromagnets will lead to a complex situation where the presence of permeable poles of electromagnet causes a large demagnetizing flux leakages through the electromagnet. Smythe used the second Maxwell's equation to predict the paths of eddy currents in a rotating conductor; Figure 7.2 from an article written by Smythe shows the lines of eddy current induced in the rotating disk by two circular magnet poles. (Smythe 1942)

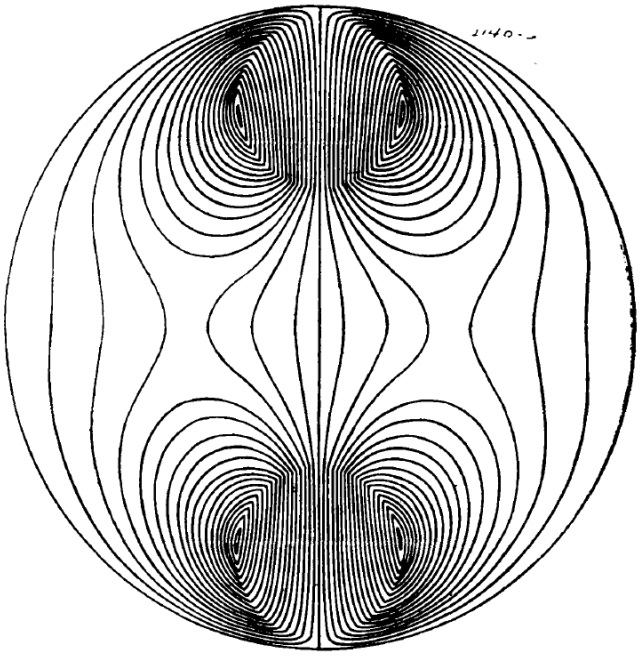

Figure 6.2. Lines of flow of eddy currents induced in rotating disk by two circular magnet poles (Smythe 1942).

In the experiment held by Smythe a disk with following parameters is utilized:

- Diameter of 100 mm
- Thickness of 4 mm

The final equation derived by Smythe can be written in the following form:

$$T = \frac{\omega\gamma R^2 \Phi_0^2 D}{(R + \beta^2\gamma^2\omega^2)^2} \times n \quad (6.5)$$

The general observation claims that with the increase in a number of poles, the torque per pole is increased taking into account demagnetizing forces (Smythe 1942)

However, Smythe (1942) also refers to Lentz graphical data to highlight the dependency between the temperature of a conductor, speed of rotation and induced braking torque as described in Figure 6.3. Additionally, it is stated that on Figure 6.3 the number of poles is four.

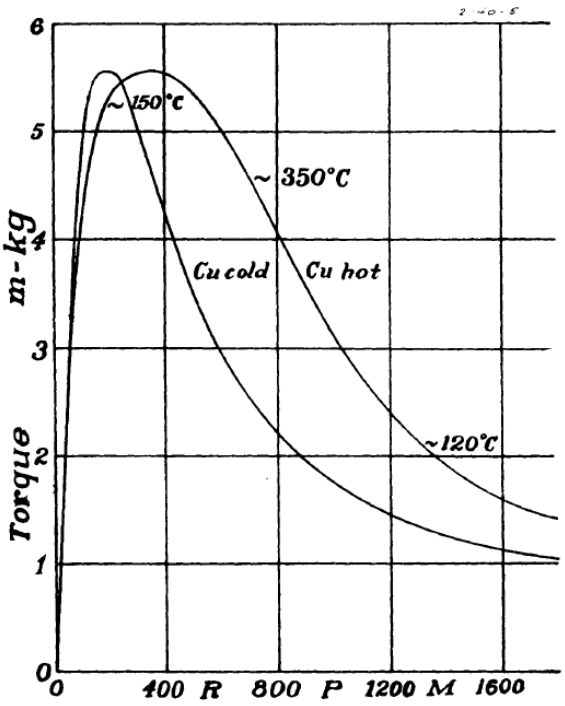

Figure 6.3. Torque versus for rotating disk between the four pole pairs of an electromagnet (Smythe 1942).

Correspondingly, Wouterse (1991) has observed the linear behavior of the braking torque at the low-speed region. After insignificant refinements, Wouterse has defined an equation for the low-speed region involving a factor C, which is meant to express the effects caused by the resistance in return paths for the eddy current and external magnetic fields.

$$F_e = \frac{1}{4}\frac{\pi}{\rho} D^2 d B_0^2 c v \quad (6.6)$$

in which:

$$c = \frac{1}{2}\left[1 - \frac{1}{4}\frac{1}{(1+\frac{R}{A})^2(\frac{A-R}{D})^2}\right] \quad (6.7)$$

Furthermore, there is a connection with the results delivered from Schieber regarding the dragging force exerted on a linearly moving strip. The factor c' can be substituted instead of c to match the linear movement condition. (Wouterse 1991)

$$c' = \frac{1}{2}\left[1 - \frac{\pi^2}{24}\left(\frac{D}{2h}\right)^2\right] \quad (6.8)$$

As it is seen from the eddy current brake sketch pictured in Figure 6.4, the magnetic flux B is generated by a coil supplied with magnetic field strength depending on the number of turns N.

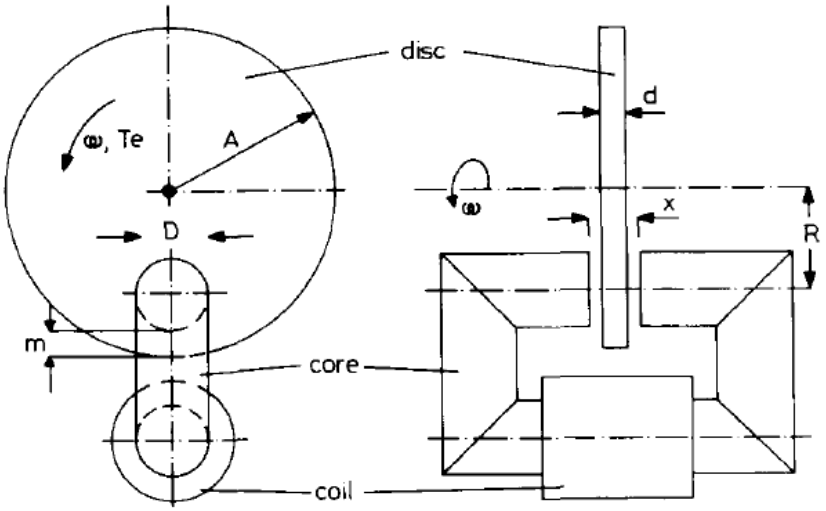

Figure 6.4. Eddy current brake (Wouterse 1991).

The result which is derived by Schieber (1974) is similar to the outcome of Wouterse with assumptions that several simplifications are required. Both, Schieber's and Smythe's models are applicable to the case with either electromagnets or permanent magnets.

$$T = \frac{1}{2}\sigma\delta\omega\pi R^2 m^2 B_z^2\left[1 - \frac{(R/a)^2}{\{1-\left(\frac{m}{a}\right)^2\}^2}\right] \quad (6.9)$$

To continue further research, the model of Wouterse was chosen due to its relative simplicity and possibility to apply its dependencies either for the low-speed region or high-speed region. Plenty of works has been done regarding optimization of processes involving eddy current brakes. Among them are Kapjin Lee & Kyihwan Park (1999), Barnes & Hardin & Gross (1993), Gosline & Hayward (2008), Simeu & Georges (1995). As an example, Barnes & Hardin & Gross (1993) apply equation 6.10 referring to the geometrical parameters of the system drawn in Figure 6.4, the idea has been taken from Wouterse's work.

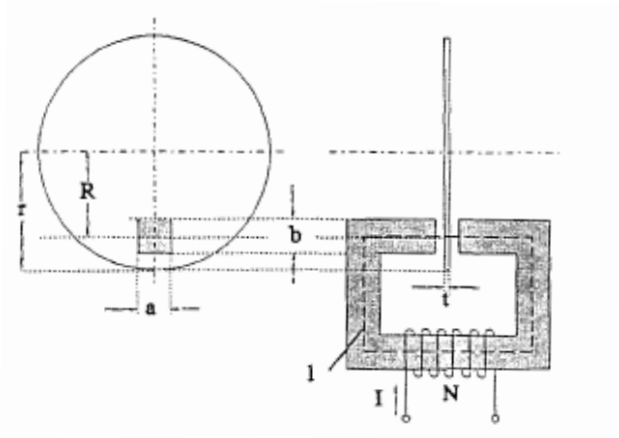

Figure 6.5. Diagram of Eddy Current Brake with variables (Barnes & Hardin & Gross 1993).

$$F = abt\sigma B_0^2 \alpha c * velocity \quad (6.10)$$

$$\alpha = 1 - \frac{1}{2\pi}\left[2\arctan(A) + a\ln\left(1 + \frac{1}{A^2}\right) - \frac{1}{A}\ln(1 + A^2)\right] \quad (6.11)$$

$$A = \frac{b}{a} \quad (6.12)$$

$$c = \frac{1}{2}\left[1 - \frac{1}{4}\frac{1}{(1 + \frac{R}{r})^2(\frac{r - R}{D})^2}\right] \quad (6.13)$$

$$D = 2\sqrt{\frac{ba}{\pi}} \quad (6.14)$$

The expression for *D* results from using a round core and represents the diameter of the equivalent circular core with the same cross-sectional area as the utilized core (Barnes & Hardin & Gross 1993).

7 Equation of motion

With a perspective to implement ECB for dumping applications, it is essential to determine the dependency of angular velocity on time. Gosline & Hayward (2008) claims that general trend is to maximize available dumping for the smallest moment of inertia. Thus, it is stated that the main aspect of ECB performance is situated within those two characteristics (Gosline & Hayward 2008).

By the condition that the friction is so small that it is neglected, the motion of ECB's rotating disk is determined by second-order differential Equation 7.1:

$$\ddot{\theta} = -\frac{b}{I}\dot{\theta} \quad (7.1)$$

, with a condition that

$$\begin{cases} \theta(0) = 0 \\ \dot{\theta}(0) = \omega_0 \end{cases} \quad (7.2)$$

Comparing Equation 7.1 to the Equation 6.1, it is mathematically evident that damping coefficient *b* is equal to:

$$b = n\,\frac{\pi\sigma}{4} D^2 d B^2 R^2 \quad (7.3)$$

Mass moment of inertia for a disk joined to 3-blade propeller is:

$$I = \frac{1}{2} m_d R^2 = \frac{1}{2} \rho \pi d R^4 \quad (7.4)$$

, where l – length of a blade, d – center of mass.

Therefore, according to Gosline & Hayward (2008) the angular velocity in dependence on time is:

$$\dot{\theta}(t) = \omega_0 e^{-\left(\frac{b}{I}\right)t} = \omega_0 e^{-\left(\frac{1}{\tau}\right)t} \quad (7.5)$$

A time constant τ is equal to the ratio of moment of inertia divided by the damping constant and appears to be a crucial characteristic of ECB's design since it covers its ability to decelerate. (Gosline & Hayward 2008).

8 Eddy current brakes application

As it has been announced earlier, the project is aimed at application of eddy current effect as a decelerating feature to the wind turbine situated near Lappeenranta University of Technology pictured in Figure 1.1.

The ECB is going to be utilized as a rotational speed controller preventing the shaft from overloading at the high range of angular velocities and ensure that the power provided by the wind is always held at sufficient levels.

One of the preliminary tasks is to determine the range of angular velocities at which ECB will operate supplying the propeller with braking torque to prevent further increase in angular speed. As it is shown in Figure 8.1, the maximum range of power initiated in the wind turbine is presented within the speed of wind ranging from 12,5 to 17 m/s. As it is known the maximum speed of the shaft is 100 RPM, which, as suggested, corresponds to the speed of the wind with a magnitude of 20 m/s. As proportional calculations were conducted, it is determined that the desirable range of angular speed is 62,5-85 RPM or 6,54-8,90 rad/s, correspondingly.

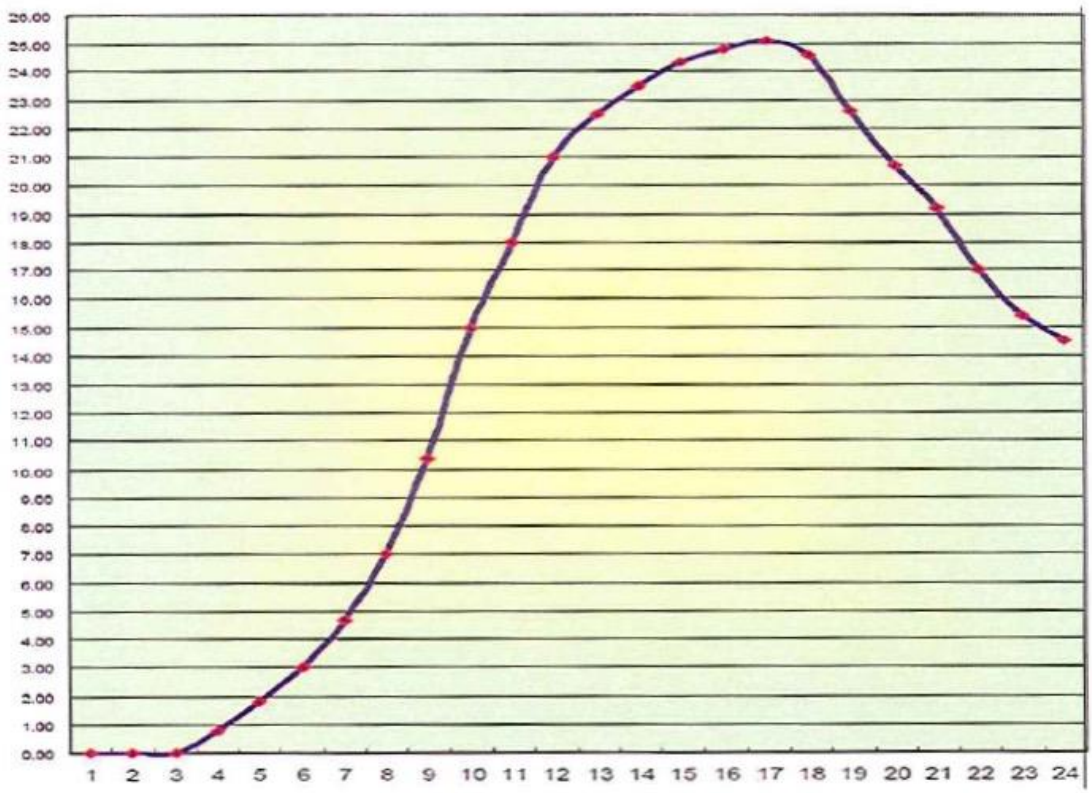

Figure 8.1 The dependency between the speed of the wind (0y) and the power of wind turbine (0x) (Marko Kasurinen – Development manager LUT).

9 Verification of deceleration magnitude and torque required

Equation 9.1 is taken to describe the system of rotational movement pictured in Figure 9.1

$$T_{wind} - T_{ECB} = -\alpha I_{total} \qquad (9.1)$$

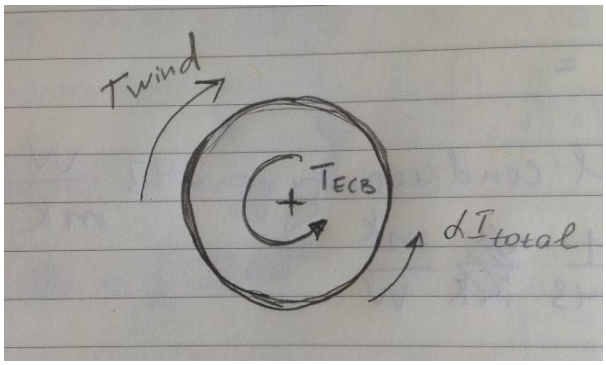

Figure 9.1. An illustration for Equation 9.1.

The system's behavior is derived to be so that the difference in the torque caused by the linear speed of the wind and braking torque of the ECB is determined by a total mass moment of inertia and desired rate of deceleration.

The total mass moment of inertia is a sum of moment of inertia of braking disk added to mass moment of inertia of propeller as shown in Equation 9.1 (Wikipedia 2016):

$$I_z = \frac{\pi \rho h}{2}(r_2^4 - r_1^4) \quad (9.2)$$

Braking disk has the following geometrical and physical characteristics, which are selected and described further in the paper:

- Outer radius 0,46 m
- Inner radius 0,2 m
- Disk thickness 0,03 m
- Disk density (Aluminum alloy) 37,4*10^6 S/m
- Disk moment of inertia I 5,5 kg*m^2

The blades are carrying the following information:

- Length 6 m
- Center mass 3 m
- Mass of a blade 64 kg
- Mass moment of inertia of the blade 768 kg*m^2
- Mass moment of inertia of the propeller 2304 kg*m^2

Therefore, the total mass moment of inertia is 2309,5 kg*m^2

To continue, the angular deceleration must be derived from the desired time of ECB operation:

- Angular speed 1 = 8,9 rad/s
- Angular speed 2 = 6,54 rad/s
- Time 15 sec.

Therefore, the angular deceleration is equal to 0,15 rad/sec^2

After processing all the data, the difference between the torques is equal to 363,36 Nm.

As the next stage, the torque caused by the speed of wind must be determined with respect to the power of propeller shown in Figure 8.1. In this case, the following equation is suggested (WENtechnology 2002):

$$T_{wind} = k * \frac{P}{\omega} \quad (9.2)$$

, where k (constant) = 9,5488, P – power (kW) and ω – angular velocity (RPM).

Angular speed, RPM	Angular speed, rad/s	Power, Watt	Torque (wind)	Torque (ECB)
85	8,90	25010	2809,6	3173,0
83,75	8,77	25010	2851,5	3214,9
82,5	8,64	25050	2899,4	3262,7
81,25	8,50	25000	2938,1	3301,5
80	8,37	24900	2972,1	3335,4
78,75	8,24	24700	2995,0	3358,3
77,5	8,11	24500	3018,7	3382,0
76,25	7,98	24400	3055,6	3419,0
75	7,85	24300	3093,8	3457,2
73,75	7,72	24100	3120,4	3483,7
72,5	7,59	23900	3147,8	3511,2
71,25	7,46	23700	3176,2	3539,6
70	7,33	23500	3205,7	3569,0
68,75	7,20	23300	3236,2	3599,5
67,5	7,07	23000	3253,7	3617,0
66,25	6,93	22800	3286,2	3649,6
65	6,80	22500	3305,4	3668,7
63,75	6,67	22400	3355,2	3718,5
62,5	6,54	22000	3361,2	3724,5

Table 9.1. The range of angular velocity with correspondence to required braking torque.

As a boundary condition, angular velocity of the shaft is divided into multiple speed range with a fix difference of 0,13 rad/s throughout the whole deceleration process from 8,9 rad/s to 6,54 rad/s as pictured in Table 9.1 Every angular velocity has its own magnitude of power, therefore, it is assumed that the torque extracted from the wind (derived with Equation 9.2) as well as the required braking torque (derived with Equation the 9.1) vary with dependency on angular speed.

10 Selection of material for rotating disk

A research aimed at investigating the effect caused by rotor's material should be started from Equation 7.5 derived by Gosline & Hayward (2008). In Equation 7.5 time constant τ is the component to express effects due to variation in system's physical, geometrical and magnetic characteristics. The suggestion is to consider the constant τ within a relationship moment of inertia and dumping coefficient in a form described in Formula 10.1:

$$\tau = \frac{I}{b} = \frac{2\rho R^2}{nD^2\sigma B^2} = \frac{\rho}{\sigma} * \frac{2R^2}{nD^2B^2} \qquad (10.1)$$

The material of the disk can affect the time constant τ and, therefore, time of braking by two of its physical characteristics, those are material's density ρ and electrical conductivity σ. In this thesis it is proposed to select an optimal material with several conditions:

- The material would have the smallest density, but the greatest rate of electrical conductivity, thus, the desired ratio of ρ to σ has to be as small as possible
- The melting temperature of a material is considered within a condition that the power dissipated by eddy currents is not able to melt the rotating disk
- The electrical conductivity of the disk should be as large as possible to expect that the critical torque is reached and applied more frequently according to Formula 6.2 as an area of application is a relatively slow rotating propeller of the wind turbine in Figure 1.1.

The first stage to select the material for the rotating disk is to identify metallic elements fulfilling the requirements after preliminary analysis and consider them by three characteristics described above, those are presented in Table 10.1.

Considered elements	
Copper Aluminum Molybdenum Zinc Lithium Tungsten	Nickel Iron Palladium Tin Lead Titanium

Table 10.1. Considered elements (TIBTECH).

Figure 10.1 illustrates graphically the results obtained from each of preliminarily selected elements. The desired relationship coefficient marked as “Ratio” is to be less than 0,5. A few of considered elements may provide the ratio which is less than 0,5. Those are Copper, Aluminum, Zinc and Lithium.

According to the temperatures which are applied to melt materials out of these elements, only Copper and Aluminum may provide a sufficient durability temperatures to melt within 1100 °C and 700 °C correspondingly.

Therefore, the most notable three alloys of Copper and nine alloys of Aluminum are compared within the requirements which were applied previously to metal elements.

Figure 10.2 shows the second stage of the analysis aimed at rotor material selection. Taking into account every requirement described earlier, it is determined that two alloys can be accepted for further consideration within known operating conditions: C10200 (Copper alloys) and UNS A91199 (Aluminum alloy), but aluminum alloy appears to be the most suitable variant to proceed with due to its density, thermal resistance, acceptable melting temperature, machinability and the price. (Table 10.2)

Alloy	Electric conductivity σ $*10^6$ S/m	Density ρ Kg/m^3*10^3	Temperature of melting (°C)
C10200	58,6	8,941	1082
UNS A91199	37,4	2,7	660

Table 10.2. Characteristics of the most suitable alloys.

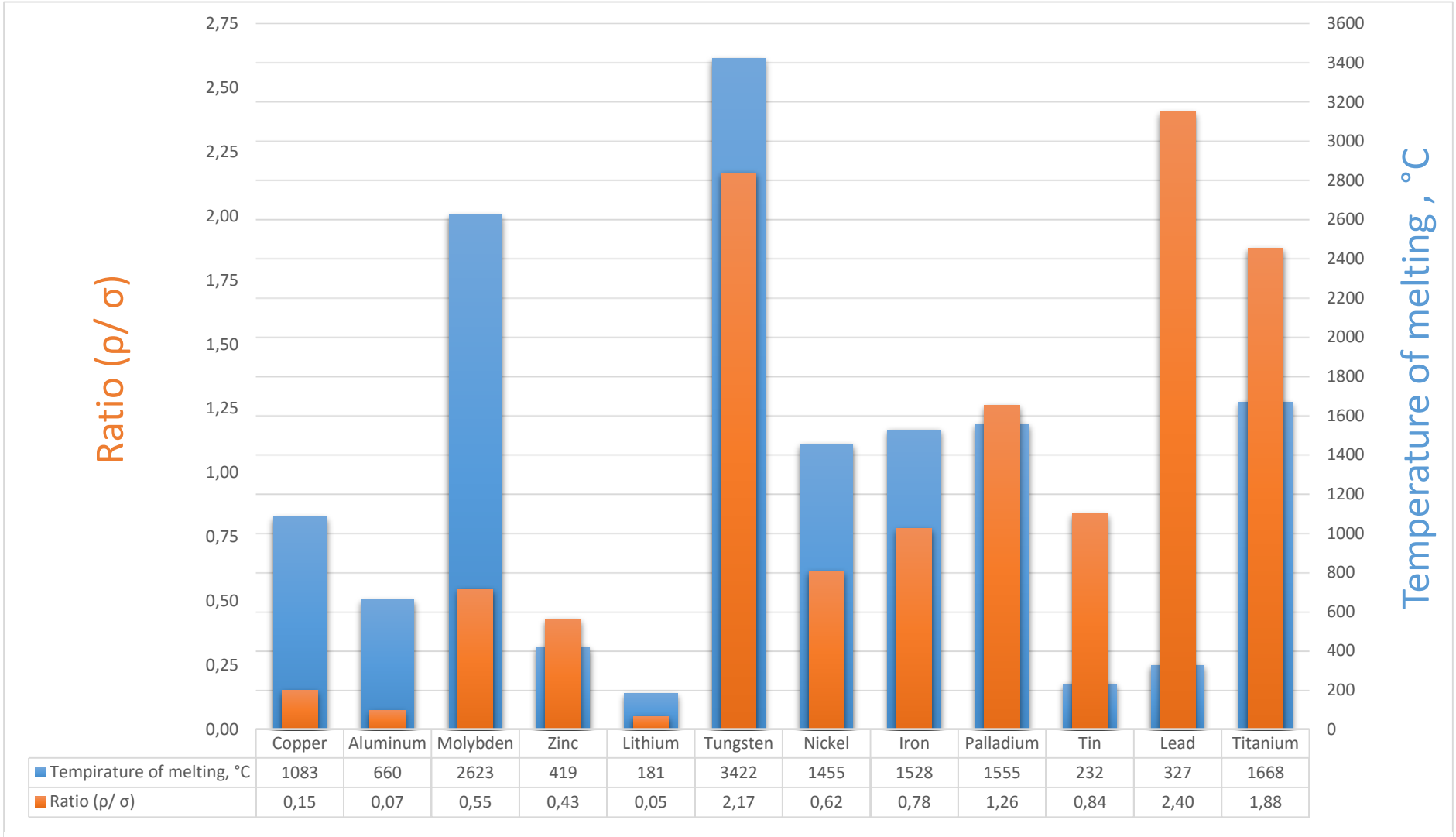

	Copper	Aluminum	Molybden	Zinc	Lithium	Tungsten	Nickel	Iron	Palladium	Tin	Lead	Titanium
Tempirature of melting, °C	1083	660	2623	419	181	3422	1455	1528	1555	232	327	1668
Ratio (ρ/ σ)	0,15	0,07	0,55	0,43	0,05	2,17	0,62	0,78	1,26	0,84	2,40	1,88

Figure 10.1. Graphic illustration of considered element's characteristics (illustrated data from TIBTECH).

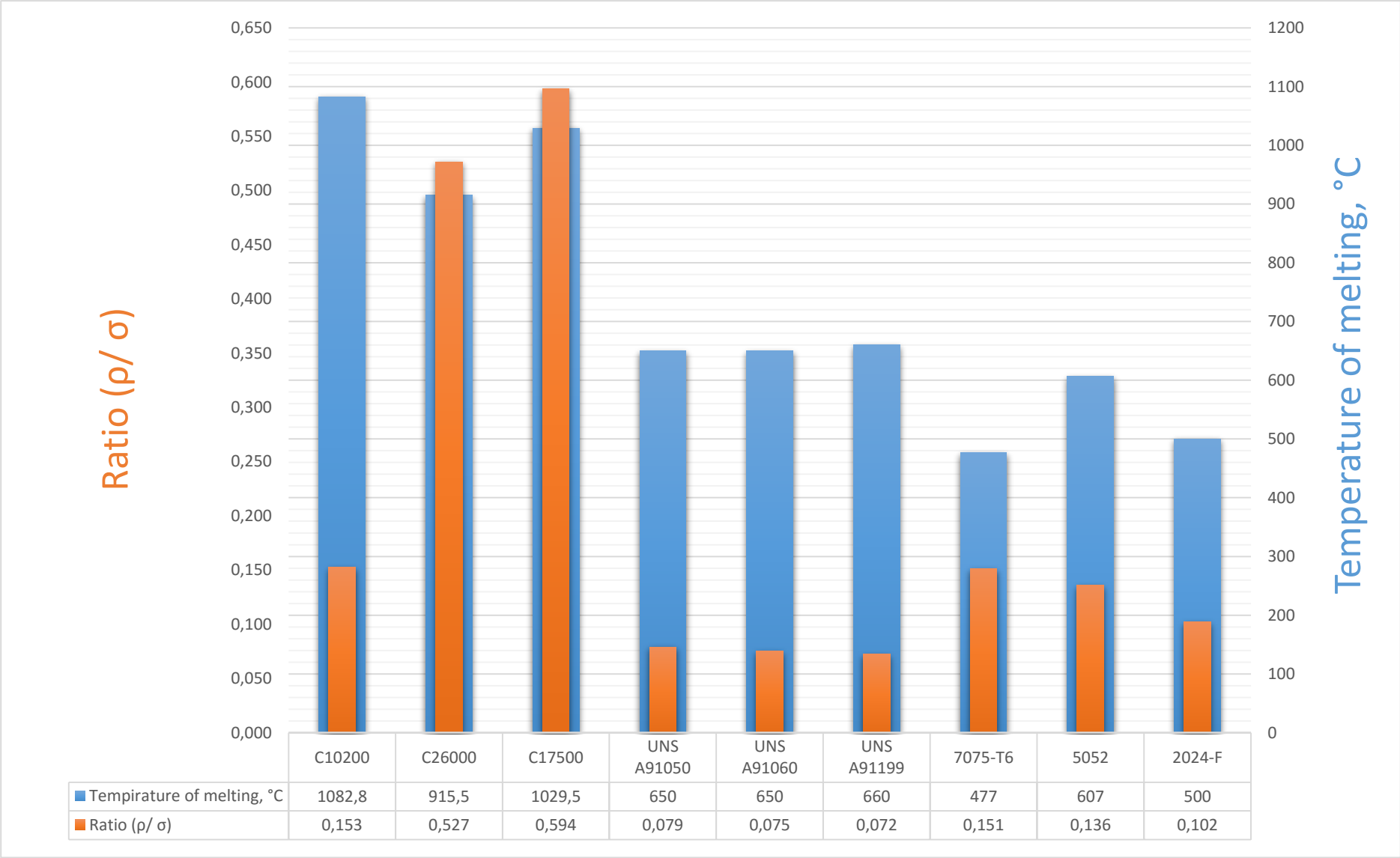

	C10200	C26000	C17500	UNS A91050	UNS A91060	UNS A91199	7075-T6	5052	2024-F
Tempirature of melting, °C	1082,8	915,5	1029,5	650	650	660	477	607	500
Ratio (ρ/ σ)	0,153	0,527	0,594	0,079	0,075	0,072	0,151	0,136	0,102

Figure 10.2. Graphic illustration of considered alloys' characteristics (Combined data from Olin Brass, Jahm, Holme Dodsworth & Collaboration for NDT Education).

11 Verification of electromagnetic characteristics

Knowing the torque required for the brake to act according to the design restrictions, the only undetermined characteristic left from Equation 6.1 is the density of magnetic field B.

The magnetic field density can be determined using Equation 5.6 and Equation 5.7 as described in Section 5.1 or based on graphical approach as it has been done in this thesis.

In this section, the material of electromagnet core is selected as the first stage. Furthermore, as the braking torque varies linearly with speed, the function of electrical current in the electromagnet is determined in relation to the angular velocity of the propeller.

11.1 Selection of electromagnet's core material

The most popular material as electromagnets core nowadays is soft iron which has outstanding features in terms of a proportional rise of magnetic field strength H to magnetic flux density B. However, three additional and highly used materials were considered within their ability to magnetize. The considered materials are:

- Cast steel
- Nickel
- Ferrite
- Soft iron

Figures 11.1-11.4 illustrate graphically the relation between the desired density of magnetic field *B* and the required intensity *H* to supply it.

Eventually, ferrite has been chosen as a primary material to implement it in the electromagnets of LUT wind turbine due to the light application circumstances where the required magnetic field strength *H* is not high and because of its crucial ability of rapid demagnetization as electrical current is not supplied.

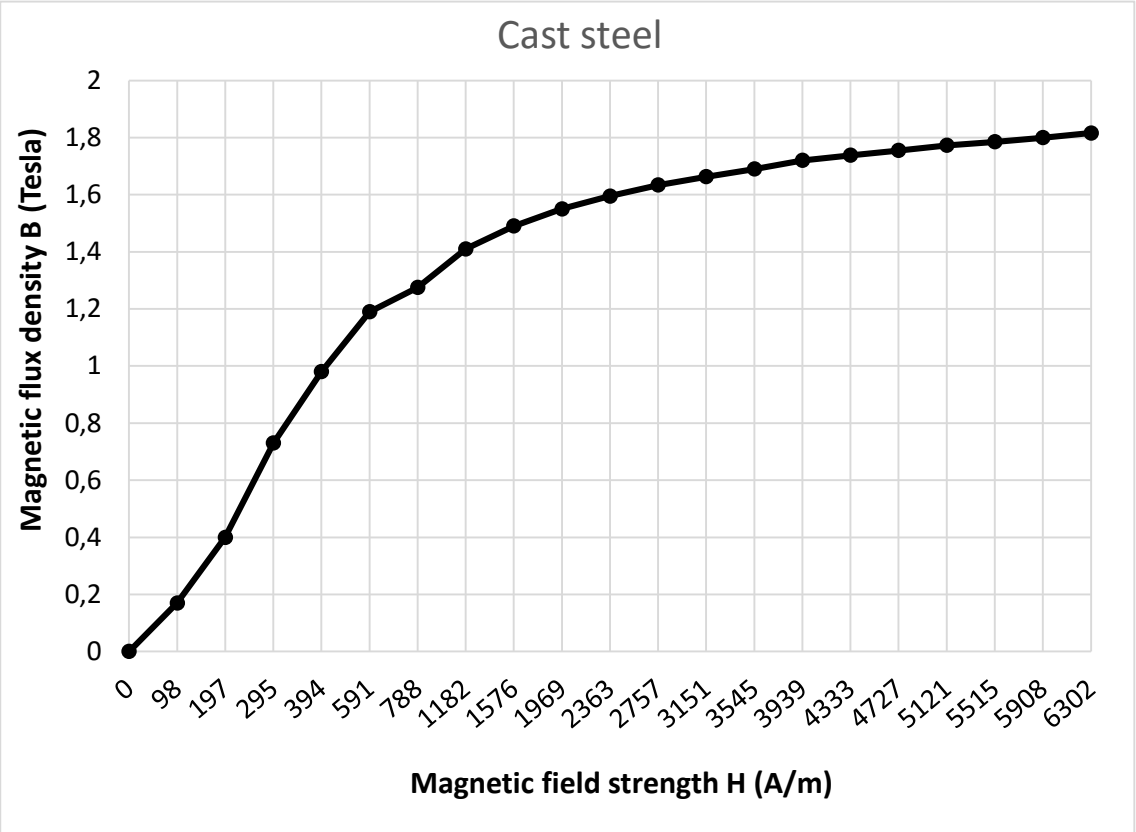

Figure 11.1. B-H curve of cast steel (Field precision LLC 2016).

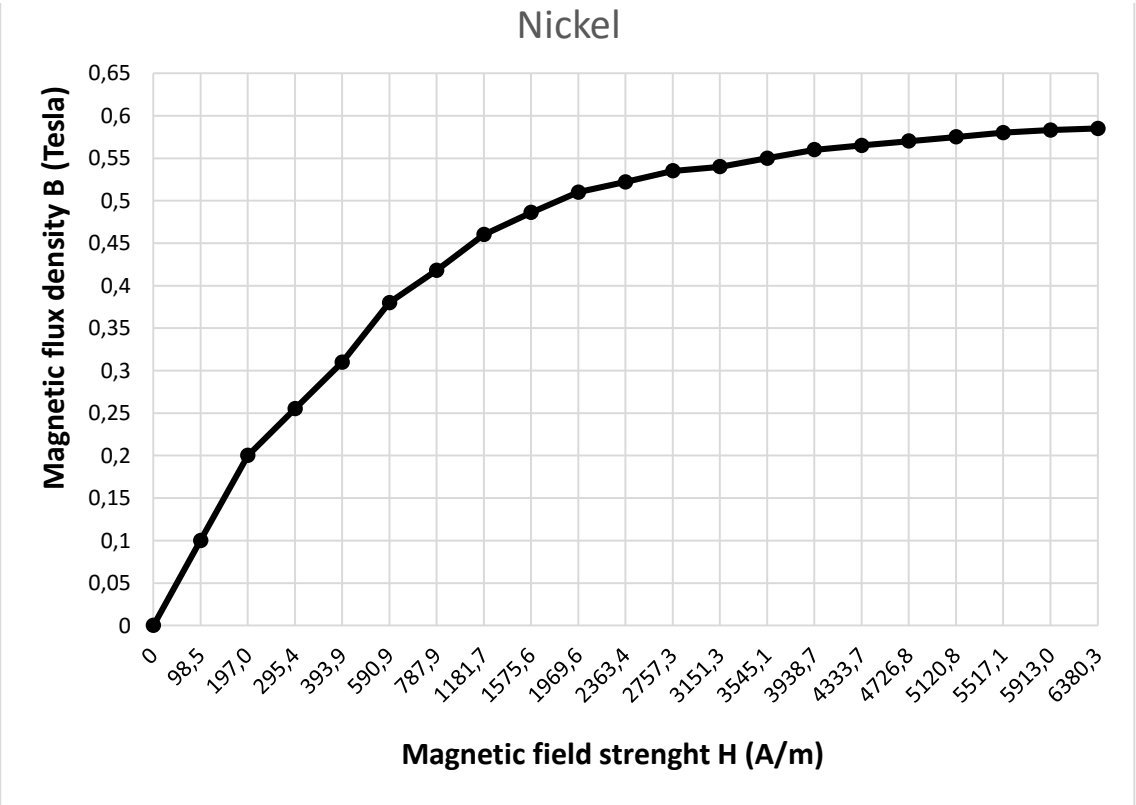

Figure 11.2. B-H curve of Nickel (Field precision LLC 2016).

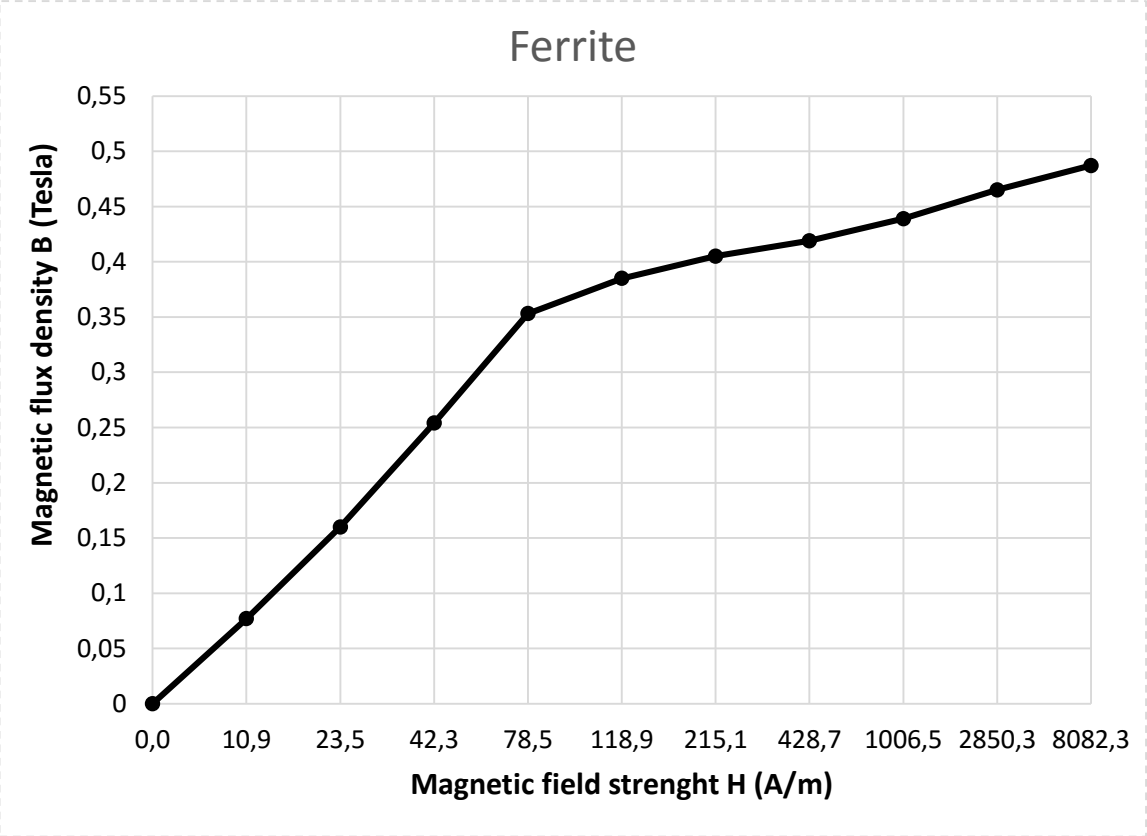

Figure 11.3. B-H curve for ferrite (Field precision LLC 2016).

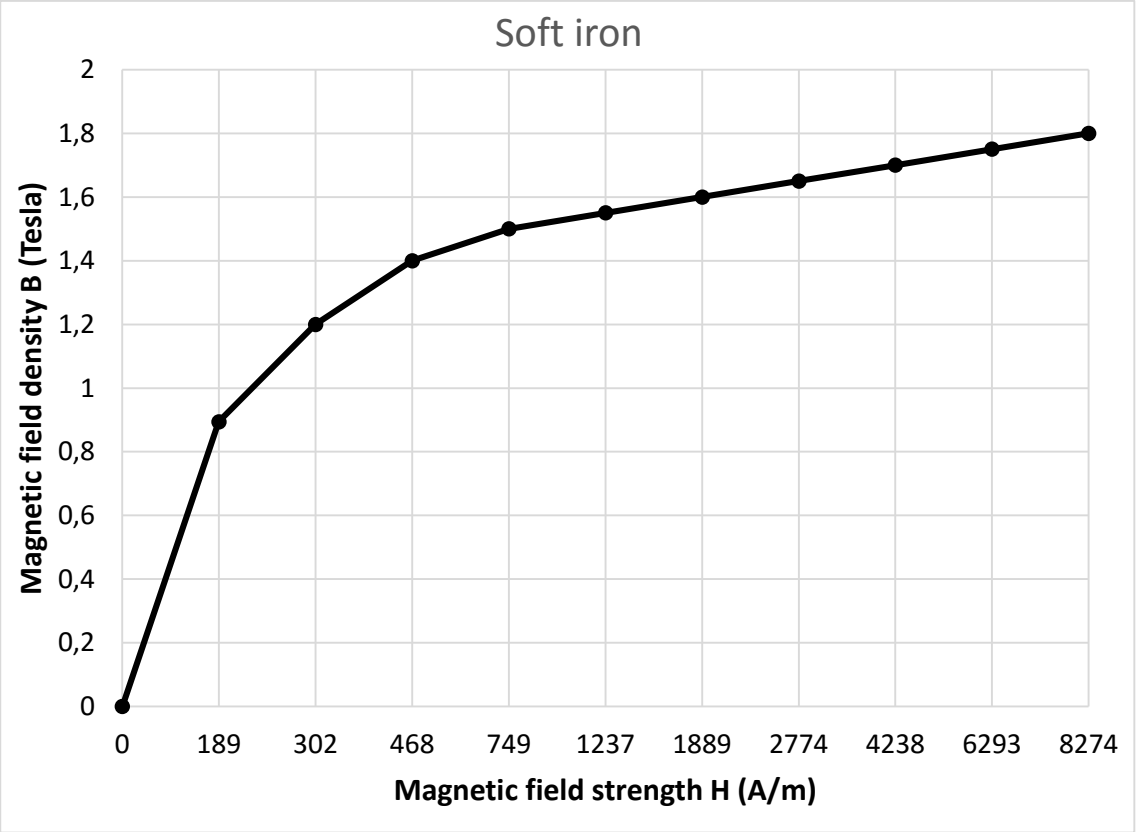

Figure 11.4. B-H curve for soft iron (Field precision LLC 2016).

11.2 Electromagnet characteristics

Electrical current is determined within the required parameters of induction and magnetic field strength presented in Table 11.1, where magnetic field strength *H* is depending on the required parameters of *B* and determined graphically from Figure 11.3.

As the magnitude of magnetic field strength is calculated, electrical current can be determined through application of Equation 5.3 from Section 5.1. Reconfigured Equation 5.3 is presented below for simplicity.

$$I = \frac{Hl}{N} \quad (11.1)$$

The required data is suggested to be taken as:

- Length of electromagnet core (l) is 10 cm
- Number of turns on electromagnet is 5
- Diameter of a core is 0,05 m

Magnetic field density, B (T)	Magnetic field strength, H (A/m)	Electrical current, I (A)
0,255	41,422	0,83
0,258	42,097	0,84
0,262	42,829	0,86
0,266	43,502	0,87
0,269	44,151	0,88
0,272	44,728	0,89
0,275	45,322	0,91
0,279	46,031	0,92
0,283	46,764	0,94
0,286	47,420	0,95

0,290	48,099	0,96
0,294	48,799	0,98
0,297	49,524	0,99
0,301	50,273	1,01
0,305	50,937	1,02
0,309	51,738	1,03
0,313	52,450	1,05
0,318	53,430	1,07
0,322	54,076	1,08

Table 11.1. The variation of electromagnetic induction with corresponding values of magnetic field strength and current.

As the current varies throughout the angular velocity of the propeller, the dependency has to be visualized. Figure 11.5 represents the total variation of electrical current needed as the propeller decelerates.

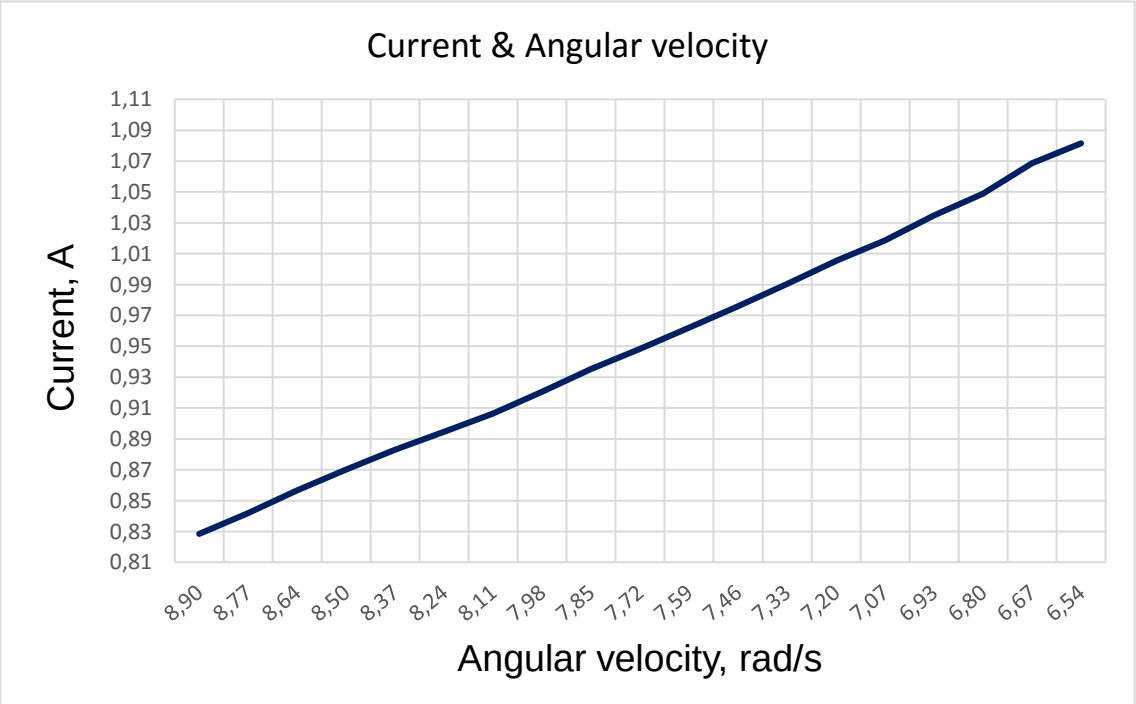

Figure 11.5. A graph presenting the variation in current value throughout the process.

12 Power and temperature dissipated by ECB

12.1 Power of ECB

The research combines the study regarding the power consumed by the aluminum disk in relation to each of the angular velocity speed sectors described in table 9.1. As the amount of dissipated power is decreasing with angular velocity throughout the whole process of deceleration, it is suggested to estimate an average power magnitude assuming that the constant value of average power is dissipated during predetermined amount of time – 15 seconds and utilize the equation 12.1 (Gosline) to approximate the rise of operating temperature and estimate the working conditions.

$$P = n\frac{\pi\sigma}{4}D^2 dB^2 R^2 \dot{\theta}^2 \quad (12.1)$$

Angular speed, rad/s	Power of ECB, kW	Angular speed, rad/s	Power of ECB, kW
8,90	28,23	7,59	26,64
8,77	28,18	7,46	26,40
8,64	28,17	7,33	26,15
8,50	28,08	7,20	25,90
8,37	27,93	7,07	25,55
8,24	27,68	6,93	25,31
8,11	27,43	6,80	24,96
7,98	27,29	6,67	24,81
7,85	27,14	6,54	24,36
7,72	26,89		

Table 12.1. The results of ECB power exerted on the disk at each of the velocity periods.

The average power of values presented in Table 12.1 is equal to 26,69 kW.

12.2 Approximation of temperate rise

The crucial characteristic of the material which is responsible for the rate of temperature increase is thermal resistance. It is often mentioned in specification sheets, therefore, it has not been found. However, there is a way to determine the thermal resistance through its physical and geometrical characteristics.

The calculation process of temperature increase starts with such a material characteristic as thermal conductivity, which shows the rate of power needed to be supplied to heat up one cubic meter of material by one degree (K or ^{o}C). The thermal conductivity of the chosen aluminum alloy is 243 W/m^{3}K.

Then, the thermal resistivity coefficient R_{ho} must be determined with a help of a magnitude of the thermal conductivity:

$$R_{ho} = \frac{1}{243}\frac{m^3 K}{W} \quad (12.2)$$

Formula 12.3 illustrates the calculation of thermal resistance *R* (Wikipedia 2016):

$$R = R_{ho}\frac{d}{A} \quad (12.3)$$

, where d is the disk's thickness and A is area perpendicular to power flow. Particularly, our variables are:

- d = 0,03 m
- A = 0,54 m^2

As a result, the thermal resistivity is 2,29*10^(-5) K/W. Therefore, it is feasible to calculate the temperature change which will be caused by applying the estimated average power. The approximate change in temperature after the deceleration from 85 to 62,5 RPM is 6,11 degrees.

13 ECB sketch and magnet configuration

Figure 13.1 introduces the preliminary location of braking disk outside the nacelle, which prevents from nacelle's rebuilding and reconfiguration of its insides.

It should be described as a circular aluminum strip with its inner and outer radiuses corresponding to the geometrical dimensions of the nacelle. The disk is attached to the blades from behind to be as close as possible to the series of electromagnets shown in Figure 13.2.

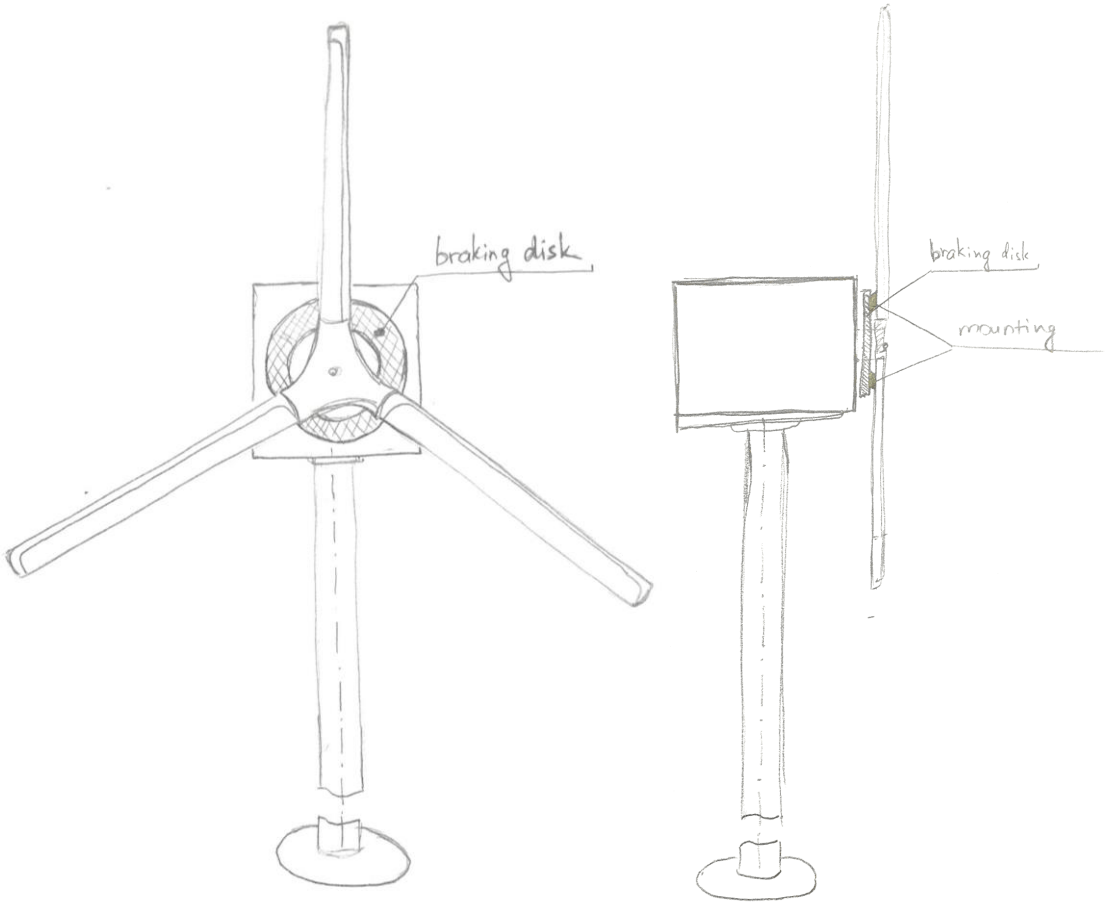

Figure 13.1 The sketch of a braking disk attached to the wind turbine.

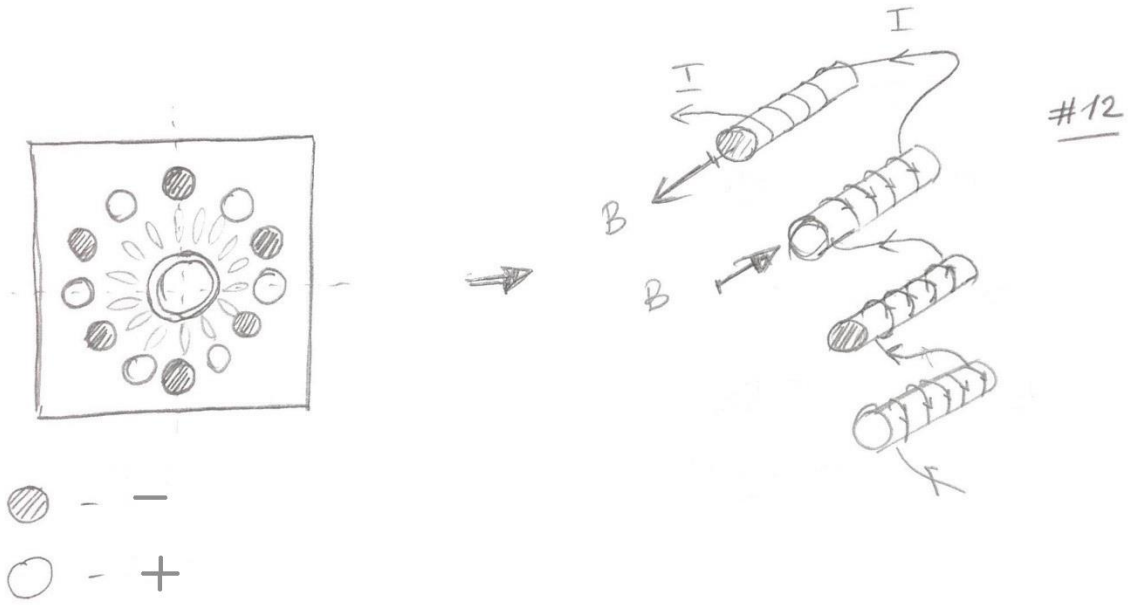

Figure 13.2 Internal construction of electromagnets with the winding.

Figure 13.2 illustrates the displacement of electromagnets, as it is seen they represent a circle right behind the braking disk from Figure 13.1. The left part of Figure 13.2 is a closer brought chain of electromagnets connected within the electrical circuit of the wind turbine. As it is shown, the marked direction of electrical current illustrates the current flow in a whole coil supplying the magnet core either with magnetic induction “out of paper” or “into the paper” as drawn. The following structure has been chosen due to its advantage over the similar pole construction as it is claimed by N. J. Caldwell and J.R.M. Taylor (Caldwell and Taylor 1998).

14 Conclusion

14.1 Summary

The primary goal of this study was to conduct an analysis of an opportunity to apply eddy current brakes in dynamical systems containing rotating shafts, explain its benefits over the conventional braking systems and seek for the similar application examples in the field of renewable energy.

In addition to that, the universal tool presented in Excel format had to be developed to introduce basic links between the system’s geometrical, electrical,

physical and magnetic characteristics and to be involved when a quick estimation is needed while any change in braking system's characteristics has been done.

While conducting the research the general principles of deceleration, eddy currents' origin, basics of magnetism and currently existing types of brakes were clarified and gathered briefly, but informatively.

The theory which is explained in this thesis was taken from reliable secondary sources. The concepts of physics were investigated from several student books presented in LUT library, however, a particular field of eddy current brake application was studied in terms of academic articles ranging from the 1940s up to the present.

Additional empirical data needed to complete the estimations of the designed system was combined following the specification sheets of various industrial companies.

The output of the research can be described as a dynamically estimated model the characteristics of which are based on a real prototype and adjusted to act effectively within prototype's environment and a fully operating Excel table being used as a tool for the system's behavior estimation in terms of a characteristic's change.

Based on the system's preliminary sketch in Figure 13.1, a general understanding of braking disk mounting and electromagnets internal organization can be studied and developed further. The numerical investigations gave a short presentation of physical and dynamical effects caused by eddy current brake operation.

14.2 Recommendations for further research

A general recommendation to continue the adaptation of ECB for the industrial use in wind turbines would be the study of structural behavior taking into account the requirement of safety. Furthermore, among the applied challenges the means of mounting are stated.

A commercial offer to apply the ECB certainly requires deeper research of a long lasting impact on the environment, costs of maintenance and efficiency of the wind turbine.

As a conclusion, the planning of industrial production is a must to enter a sector in a market of sustainable technologies with further product development and innovation.

Figures

Tables

References

AK steel Corporation. 444 Stainless steel. http://www.aksteel.com/pdf/markets_products/stainless/ferritic/444_data_sheet.pdf. Accessed on 3 March 2016.

Alonso M. and Finn E. J. 1992. Physics. pp. 715-727. Accessed on 21 January 2016.

Barnes, L. Hardin, J. Gross, C. 1993. An Eddy Current Braking System. IEEE, pp. 58-62. Accessed on 3 February 2016.

Bird, J. 2014. Electrical circuit theory and technology, fifth edition. Bell & Bain Ltd, Glasgow, Great Britain. Accessed on 29 January 2016.

Caldwell, N.J. Taylor, J.R.M. 1998. Eddy-Current Actuator for a Variable Pitch Air Turbine. Proc. Third European Wave Power Conference, Patras. Accessed on 3 February 2016.

Coastersandmore. 2010. Achterbahnbremsen - Von der Reib - zur Wirbelstrombremse. http://www.coastersandmore.de/rides/brake/brake.shtml. Accessed on 27 January 2016.

Collaboration for NDT Education. 2002. Conductivity and Resistivity Values for Aluminum & Alloys. https://www.nde-ed.org/GeneralResources/MaterialProperties/ET/Conductivity_Al.pdf. Accessed on 3 March 2016.

Fishbane, P. M., 1996. Physics for scientists and engineers. Second Edition. Upper Saddle River, N.J., Prentice Hall. Vol. II pp. 837-863. Accessed on 21 January 2016.

Field Precision LLC. 2016. Saturation curves for soft magnetic materials. http://www.fieldp.com/msat.html. Accessed on 3 March 2016.

Gosline, A. Hayward, V. 2008. Eddy Current Brakes for Haptic Interfaces: Design, Identification, and Control. Mechatronics, IEEE/ASME Transactions on, vol. 13. pp. 669-677. Accessed on 3 February 2016.

Guru B.S. and Hiziroglu H.R. 1998. Electromagnetic Field Theory Fundamentals. Accessed on 18 January 2016.

Holme Dodsworth. 2016. The data sheet for aluminum alloy UNS A91050. http://www.holmedodsworth.com/materials/datasheets/aluminium-datasheets/1050A-Aluminium. Accessed on 3 March 2016.

JAHM Software. 2016. The properties and materials. https://www.jahm.com/pages/property_list_props.html#SIGMA. Accessed on 3 March 2016.

Lee, K. Park, K. 1999. Optimal robust control of a contactless brake system using an eddy current, pp. 615-631. Elsevier Science Ltd. Accessed on 3 February 2016.

Mac C. June 2014. The design of an electrically controlled eddy current brake. Charles Darwin University. Accessed on 18 January 2016.

Olin Brass. 2016. C10200 alloy data sheet. http://www.olinbrass.com/resources/alloy-data-specifications/C10200-(ASTM-B152)-Oxygen-Free-Copper. Accessed on 3 March 2016.

Ozolin A. 2009. Tormozhenie mashin i mechanismov systemami s postoyannymi magnitami (Braking of machines and mechanisms with systems of permanent magnets). State Polytechnic University. Accessed on 19 January 2016.

Physbook. 2011. Magnitude pole (Magnetic field). http://www.physbook.ru/index.php/%D0%9A%D0%A1._%D0%9C%D0%B0%D0%B3%D0%BD%D0%B8%D1%82%D0%BD%D0%BE%D0%B5_%D0%BF%D0%BE%D0%BB%D0%B5. Accessed on 19 January 2016.

Schieber, D. 1974. Braking torque on rotating sheet in stationary magnetic field. PROC. IEE, Vol. 121, No.2. Accessed on 3 February 2016.

Simeu, E. Georges, D. 1995. Modeling and control of an eddy current brake. Control Engineering Practice vol. 4, pp. 19-26. Accessed on 3 February 2016.

Smythe, W. R. 1942. On eddy currents in a rotating disk. Electrical Engineering, vol. 61, pp. 681-684. Accessed on 3 February 2016.

Tipler P. A. 1990. Physics for scientists and engineers. New York, NY, Worth Publishers: 1990. pp 656-1021 Accessed on 21 January 2016.

TIBTECH. Properties table of Stainless steel, Metals and other Conductive materials. http://www.tibtech.com/conductivity.php. Accessed on 3 March 2016

WENtechnology. 2002. http://www.wentec.com/unipower/calculators/power_torque.asp. WEN Technology Inc., Raleigh, NC 27616 USA. Accessed on 3 March 2016.

Wikipedia. 2016. Alternating current. https://en.wikipedia.org/wiki/Alternating_current. Accessed on 22 January 2016.

Wikipedia. 2016. Eddy current brakes. https://en.wikipedia.org/wiki/Eddy_current_brake. Accessed on 27 January 2016.

Wikipedia. 2016. Electromagnetic induction. https://en.wikipedia.org/wiki/Electromagnetic_induction. Accessed on 2 February 2016.

Wikipedia. 2016. Inductance. https://en.wikipedia.org/wiki/Inductance. Accessed on 2 February 2016.

Wikipedia. 2016. Permeability (electromagnetism). https://en.wikipedia.org/wiki/Permeability_%28electromagnetism%29. Accessed on 2 February 2016.

Wikipedia. 2016. Right-hand rule. https://en.wikipedia.org/wiki/Right-hand_rule. Accessed on 22 January 2016.

Wikipedia. 2016. Saturation. https://en.wikipedia.org/wiki/Saturation_%28magnetic%29. Accessed on 2 February 2016.

Wikipedia. 2016. The list of moments of inertia. https://en.wikipedia.org/wiki/List_of_moments_of_inertia. Accessed on 1 March 2016.

Wikipedia. 2016. Thermal resistance. https://en.wikipedia.org/wiki/Thermal_resistance. Accessed on 5 March 2016.

Wind Power. Lappeenranta University of Technology. http://www.lut.fi/web/en/green-campus/green-energy-and-technology/wind-turbine. Accessed on 27 January 2016.

Wouterse, J. H. 1991. Critical torque and speed of eddy current brake with widely separated soft iron poles. Electric Power Applications, IEE Proceedings B, vol. 138, pp. 153-158. Accessed on 3 February 2016